BATCH vs. CONTINUOUS CRYSTALLIZATION:

THE EFFECT OF METHODOLOGY ON GYPSUM CRYSTALS FEATURES.

Versiane Albis Leão[1], Virgínia, S. T. Ciminelli[2]; Sônia D. F. Rocha[3]

[1]Mestre, Departamento de Eng. Metalúrgica - UFOP. Praça Tirandentes, 20; Ouro Preto, MG. Tel.: 0055-31- 5591561. Fax.: 0055-31-5511988. @mail: versianc@em.ufop.br

[2]MSc, PhD, Departamento de Eng. Metalúrgica-UFMG.

[3]Mestre, Departamento de Eng. Química UFMG.

Abstract:

The effect of impurities and seed addition during $CaSO_4.2H_2O$ precipitation in phosphoric acid solutions have been investigated. The differences in results obtained using batch and continuous systems are discussed and correlated to the distinct nucleation mechanisms that predominate in both regime.

Resumo

Investigou-se o efeito de impurezas e da adição de sementes durante a precipitação do $CaSO_4.2H_2O$ em soluções de ácido fosfórico. As diferenças observadas nos ensaios contínuos e em batelada foram analisadas e correlacionadas com o mecanismo predominante de nucleação nos dois sistemas.

Key-Words: Gypsum, Crystallization, Precipitation, Nucleation, Phosphogypsum.

Introduction:

Many techniques have been used to investigate crystallization processes and mechanisms. Methods as batch precipitation at low and high constant supersaturations, in the presence and absence of seeds; continuous experiments carried out in MSMPR reactors; stopped-flow techniques; determination of induction times, among others, are reported in the literature. Nevertheless, even the same experimental technique has led to contradictory results with respect to crystal sizes and morphology [1].

In a previous work, aimed at improving the performance of solid/liquid separation step in the phosphoric acid production, the effect of impurities, added as Al_2O_3, Fe_2O_3, MgO, on calcium sulfate dihydrate (gypsum) morphology (size and length [L]/width [W] ratio) has been investigated [2]. The experiments have been carried out in a batch reactor. The present work presents the results obtained in a MSMPR continuous cristallizer and compare them with those obtained in a batch system. The differences in results obtained in these systems are correlated to the distinct nucleation mechanisms that predominate in both regimes.

The thermodynamic driving force for nucleation from aqueous solutions can be represented by the gradient between the chemical potential ($\Delta\mu$) in the liquid and in the solid phases:

$$(\Delta\mu) = kT\ln(a/a_e) = kT\ln(c/c_e) \qquad (1)$$

where a is activity, c is concentration, T is temperature and k is the Boltzmann constant. The subscript e denotes equilibrium conditions.

The above expression indicates that the driving force for nucleation is a logarithmic function of the ratio between the solute activities in the actual and in the equilibrium (saturated) solutions. This ratio defines supersaturation (S). A spontaneous nucleation occurs when $\Delta\mu>0$, thus implying that $S> 1$, i.e., the solution is supersaturated with respect to the solute ($a>a_e$).

The Gibbs free energy necessary to precipitate a solid from solution is represented by [3]:

$$\Delta G_{het} = - n\Delta\mu + \phi(n) \qquad (2)$$

where n is the number of monomers[1] and $\phi(n)$ is the surface energy term involving surface area and surface tension (σ).

[1]Monomer is the smaller entity that incorporate to crystal

Taking into consideration the formation of a spherical particle, equation (2), becomes:

$$\Delta G = - (4\pi r^3/v_a)\Delta\mu + 4\pi r^2\sigma \qquad (3)$$

with r being the cluster radius and v_a, the monomer volume.

Eq. (3) shows an inflection at one specific r value (figure 1). This value, known as critical radius, r^*, is represented by:

$$r^* = 2\sigma v_a/\Delta\mu \qquad (4)$$

The monomer number (n^*) on a cluster with a critical radius is given by:

$$n^* = [2\sigma a/3\Delta\mu]^2 \qquad (5)$$

where *a* is the surface area of a monomer.

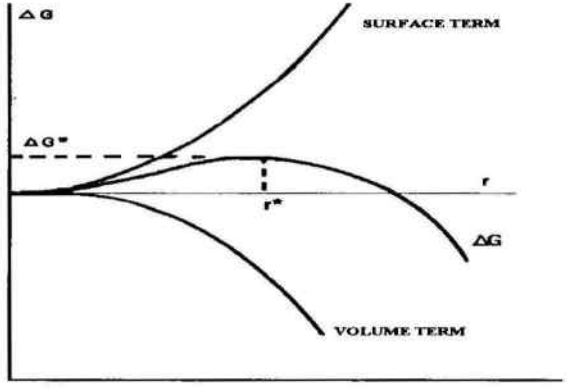

Figure 1: Gibbs free energy as a function of the cluster radius.

Crystal growth will occur when the cluster radius becomes larger than the critical radius. For this situation, there is a decrease in the Gibbs free energy. Clusters having smaller radius than the critical one will redissolve.

The cluster size distribution (C_n) follows the Boltzmann distribution model:

$$C_n = C_0 \exp (-\Delta G/RT) \qquad (6)$$

a) Primary homogeneous nucleation:

The variation in the number of clusters in a system with volume V, during a time interval, is the nucleation rate (J).

$$J(t) = Vdn/dt \qquad (7)$$

Three mechanisms of nucleation may occur in a precipitation system: (a) primary homogeneous nucleation, when there is no particle for deposition of precipitants; (b) primary heterogeneous nucleation, when solute precipitation occurs at a foreign surface (other than of solute) and (c) secondary nucleation, when deposition occurs on seeds of the precipitant. Secondary nucleation will be further examined in this paper.

When J(t) is calculated for conditions of constant supersaturation ($\Delta\mu$) in systems where homogeneous nucleation predominates, the following expression is obtained:

$$J(s) = zf^*_{homo}C^*_{homo} \qquad (8)$$

J(s) is called *stationary nucleation rate*.

Term z is called the *Zeldovich factor* and shows the number of critical nuclei (n^*) that tend to growth. From a practical point of view, $z = f(\Delta\mu)$, shows a negligible variation as compared to the other terms in equation (8). f^* represents the frequency of monomers incorporation to the critical nuclei and C^* indicates the nuclei concentration. Applied to spheres, equation (8) becomes:

$$J(s) = A'Sexp[16v_a^2\sigma^3)/(3RTln^2S) \qquad (9)$$

b) Primary heterogeneous nucleation:

While homogeneous nucleation occurs in pure solution and at high supersaturations, heterogeneous nucleation occurs frequently at low supersaturations, favored by the affinity between solute and particles present at the reactor (other than the precipitating solids). In this case, the nuclei forms a contact angle, θ, with the substrate, as shown in figure 2.

As for homogeneous nucleation, the Gibbs free energy for heterogeneous nucleation may be written as:

$$\Delta G_{het} = - n\Delta\mu + \phi(n) \qquad (10)$$

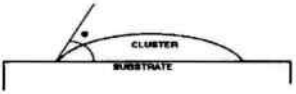

Figure 2: Contact angle between nuclei and substrate.

By applying equation (3) to the system outlined in figure 2:

$$\phi(n) = [(1/2)\,(1-\cos\theta) - (1/4)\mathrm{sen}^2\theta\cos\theta]4\pi r^2\sigma = \Psi(\theta).4\pi r^2\sigma \qquad (11)$$

$\Psi(\theta)$ is also defined as the ratio of volume of cap-shaped segment and the volume of the sphere with radius r:

$$\Psi(\theta) = (v_a n)/(4/3\pi r^3) \qquad (12)$$

The Gibbs free energy for heterogeneous nucleation is represented by:

$$\Delta G_{het} = -(4\pi r^3/v_a)\Delta\mu + \Psi(\theta).4\pi r^2\sigma \qquad (13)$$

and, by substituting equation (13) on equation (2):

$$\Delta G_{het} = \Psi(\theta).\Delta G_{homo} \qquad (14)$$

By equation (14), is may be seen that the Gibbs free energy for heterogeneous nucleation is a function of the contact angle, θ.

The presence of different substrates affect the nucleation kinetics. The stationary nucleation rate J(s) under heterogeneous nucleation conditions may be represented by:

$$J(s) = J(s) = zf^*_{het}C^*_{het} \qquad (15)$$

The heterogeneous nucleation does not alter the Zeldovitch factor, z, because this factor only represents the probability of a cluster jump the critical radius barrier.

The relationship between f^*_{het} and f^*_{homo} is given by:

$$f^*_{het} = \Psi(\theta).f^*_{homo} \qquad (16)$$

As $0 \leq \Psi(\theta) \leq 1$, it may seen that:

$$f^*_{het} \leq f^*_{homo} \qquad (17)$$

The critical nuclei concentration, C^*_{het}, is related to the nuclei concentration at equilibrium C_0:

$$C_{0,het} = \text{constant} \times \exp(-\Delta G^*_{het}/kT) \qquad (18)$$

or:

$$C_{0,het} = \text{constant} \times \exp(-\Psi(\theta).\Delta G_{homo}/kT) \qquad (19)$$

As $\exp(-\Psi(\theta).\Delta G_{homo}/kT) > \exp(-\Delta G_{homo}/kT)$ when $0 \leq \Psi(\theta) \leq 1$, two opposing factors affect the nucleation rate. The decrease of the energy barrier leads to an increase of nucleation rate whereas the decrease of the incorporation frequency decreases the value of that property. The final result depends on the level of supersaturation. At low supersaturations, $J_{het} \geq J_{homo}$ owing to the major effect of the exponential term of equation (19). At high supersaturations, $J_{het} \leq J_{homo}$ because of frequency term (equation (17)) predominates (figure 3).

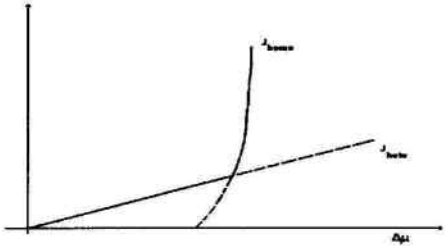

Figure 3. Nucleation rate variation in function of $\Delta\mu$.

Taking into consideration a spherical geometry, the expression for stationary heterogeneous nucleation rate becomes:

$$J(s) = A'Sexp[16v_a^2\sigma^3)/(3RTlnS) \qquad (20)$$

Continuous crystallization:

Few equations developed for continuous crystallization will be presented in the following paragraphs. More details may be found in a previous publication [4].

The kinetics of continuous crystallization in MSMPR reactors can be represented by the following equation:

$$n(L) = n_0 \exp(-l/G\tau) \qquad (21)$$

where G is the growth rate, n(L) is the population density, τ is the residence time and n_0 is the population density at L=0 (nuclei). A plot of ln(*n*) versus L features a straight line with slope equal to (-1/Gτ) and intercept equal to n_0 (Figure 4). Knowing the residence time (τ) and growth rate (G), n_0 can be determined. The nucleation rate, B_0, is related to the growth rate through eq.(22):

$$B_0 = n_0 G \qquad (22)$$

Experimental procedure

Batch experiments

Batch experiments were carried out in a 1000 ml stirred glass reactor immersed in a thermostatic water bath. Temperature was kept at 70 °C. A phosphoric/sulfuric acid solution (28,0% de P_2O_5 and 15,2% de H_2SO_4) was continuously added, at a flow rate of 0,36 ± 0,05 g/min (total addition: 100g) to a vessel containing 500g of monocalcic phosphate solution (0,8% de CaO and 28% de P_2O_5) and the desired additive concentration. 0,5 g of calcium sulfate dihydrate were used as seeds. By the end of 6 hours, the pulp was vacuum filtered, crystals were acetone washed and dried at room temperature for 24 hours. A detailed methodology is described in previous works (Rocha and Ciminelli, 1992 ,1994; Leão and Ciminelli, 1992).

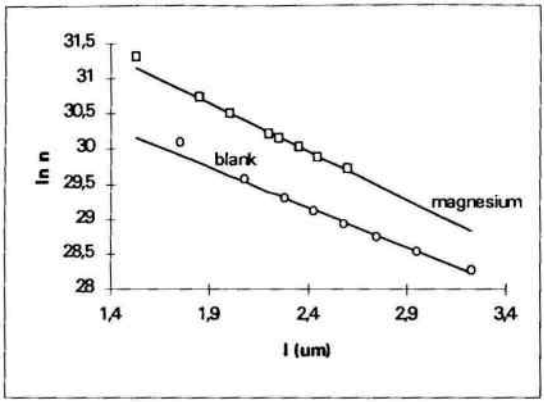

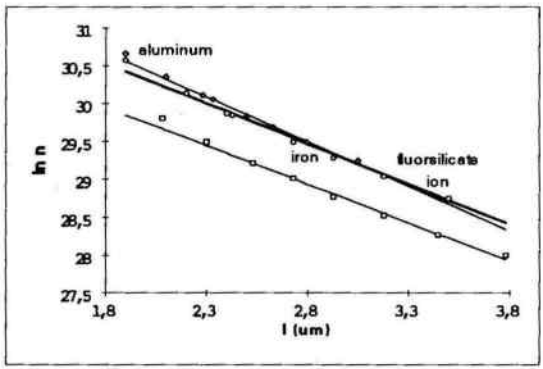

Figure 4.: Determination of growth and nucleation rates of gypsum crystals.

Continuous experiments

Continuous experiments were carried out in a MSMPR ("Mixed Suspension Mixed Product Removal") reactor. Two peristaltic pumps promoted the addition of monocalcic phosphate solution (0,8% de CaO, 28% P_2O_5 and additive) and sulfuric acid (20% H_2SO_4, 28% P_2O_5) to the reactor. The system operated at residence time of 1h and 50 min and temperature of 70 ^{o}C. Total reaction time was fixed in 10 hours.

Pulp density, pH, liquid phase density, sulfate and phosphorous concentrations were assayed at 2, 6, 8, and 10 hours. At the end of the experiments the solids were filtered and dried according to the procedure described for the batch experiments. All experiments were carried out with distilled water and reagent grade chemicals.

Solid characterization and chemical analyses

Solid phase identification was done by X-ray diffraction analysis (Phillips model PW 1400). Crystal sizes were measured by two techniques. The equivalent diameter or Stokes diameter (d_{50}) was determined by Sedigraph, model 5000ET (Micromeritics Corp. Inst.). The average crystal length (L) and width (W) were measured from SEM (Scanning Electron Microscope, Jeol JSM 35C) micrographs. P_2O_5 concentration was colorimetrically determined; sulfate levels were assayed by turbidimetry after precipitation of $BaSO_4$.

Results and discussion:

During precipitation there is a competition of kinetic phenomena involving nucleation, growth and agglomeration. The precipitate features are determined by the relative importance of each phenomenon.

Batch precipitation is a transient process and because of this, yields nucleation and growth rates that change with time. So, distinct phenomena may predominate as the reaction proceeds. Even the sequence adopted for the addition of reagents may be relevant. If the precipitation species is joined to a solution containing the cation to be precipitated, supersaturation is kept low (direct precipitation). If the cation to be precipitated is joined to the precipitant solution (inverse precipitation), high levels of supersaturation are achieved. Different nucleation mechanisms prevail in both systems and may affect the characteristics of the solid precipitate [7]. Otherwise, continuous crystallization is a steady state process. After the initial transient period , the conditions remain constant. This situation resembles those found in industrial operations.

Table I shows the different sizes and morphology of solids precipitated in batch and in continuous reactors. Pictures of gypsum crystals (blank experiments) depicted in Figure 5 indicate the smaller L/W ratio for precipitation in batch reactor as compared to that observed in continuous operation.

The addition of aluminum and magnesium affected gypsum crystal sizes, length and L/W ratios. Aluminum caused the most significant increase in crystal sizes and decrease in L/W ratio, thus confirming some results previously reported in the literature [8]. In the presence of magnesium and fluorsilicic acid, crystal sizes are reduced while iron showed no effect [2]. Similar trends were not observed when the precipitation was carried out in continuous system.

Table I. Dimensions of crystals precipitated under batch and continuous conditions.

Impurity	Batch			Continuous		
	d_{50}	C(μm)	L/W	d_{50}	C(μm)	L/W
blank	35	361	10,9	25	428	25,3
0,2% MgO	24	155	11,4	22	398	22,2
0,05% Al_2O_3	42	364	07,3	25	425	24,6
0,05% SiF_6^{-2}	16	195	10,2	26	431	24,7
0,8% Fe_2O_3	36	334	13,4	28	467	27,5

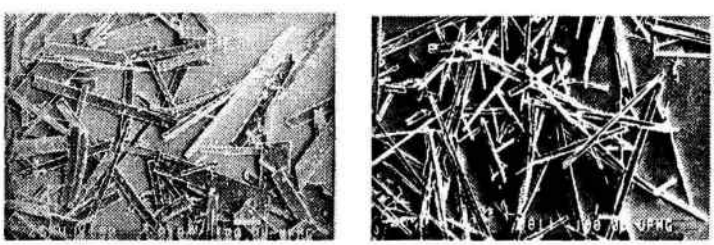

Figure 5. Gypsum crystals precipitated in batch (a) and continuous (b) systems.(100X, white bars represent a 100 μm length).

Although the impurity concentration tested in the continuous system has been chosen as that causing the most significant variation in the batch experiments, the crystal size and L/W ratios were not altered in the former. The application of MSMPR modeling to these results confirms that crystal growth and nucleation rates are of the same order of magnitude (table II and figure 4), regardless the presence or absence of the impurity.

Table II.: Growth rate, nucleation rate and initial crystals number determined from MSMPR modeling applied to gypsum precipitation

Impurity	n_0 (#/m^4)	G (m/s)	B_0[#/(m^{3}s)]
blank	$1,47 \times 10^{14}$	$1,32 \times 10^{-7}$	$1,95 \times 10^{7}$
MgO	$2,71 \times 10^{14}$	$1,11 \times 10^{-7}$	$3,01 \times 10^{7}$
Al_2O_3	$1,23 \times 10^{14}$	$1,42 \times 10^{-7}$	$1,74 \times 10^{7}$
SiF_6^{-2}	$1,35 \times 10^{14}$	$1,29 \times 10^{-7}$	$1,75 \times 10^{7}$
Fe_2O_3	$0,62 \times 10^{14}$	$1,50 \times 10^{-7}$	$0,94 \times 10^{7}$

The differences observed in crystal sizes yielded in batch and continuous precipitation systems by the impurities effect may bee partially explained by the different supersaturation levels maintained in both regimes.

Figure 6 shows the d_{50} of crystals precipitated in batch systems when the time lag between the beginning of the experiment and seed addition (related to the saturation level in the reactor) has been varied. The addition of seeds on "0" level of supersaturation yields very small crystals. In this situation, the presence of low concentrations of impurities plays an important role. The addition of 0,05% Al_2O_3 raises d_{50} from 5 to 22 (about 350% growth). When the addition of seeds is carried out under higher supersaturation levels, the precipitates become larger while the effect of impurities becomes less evident. Now, the increase of gypsum crystal size at 0,05% Al_2O_3 concentration is smaller (only 26%) and becomes negligible at even higher supersaturation levels (figures 6(b) and 6(c)).

Figure 7 depicts the differences in sizes of crystals precipitated under distinct impurities concentration, at a constant supersaturation level. It may be seen that crystals precipitated at low aluminum concentrations are larger than those obtained at higher concentrations, as shown in figure 6. The effect of impurities may be associated to their influence on the solubility of the calcium sulfate. It is known that the variation of ionic strength changes solubility and, consequently, alters the supersaturation (S) and interfacial tension (σ). He et all [8,9] showed that, in NaCl - $CaSO_4$ solutions, increasing ionic strength increases the growth rate of gypsum up to 3 molal of NaCl as background electrolyte, owing to a larger calcium sulfate solubility. Above this value, the growth rate decreases due to the reduction of solubility.

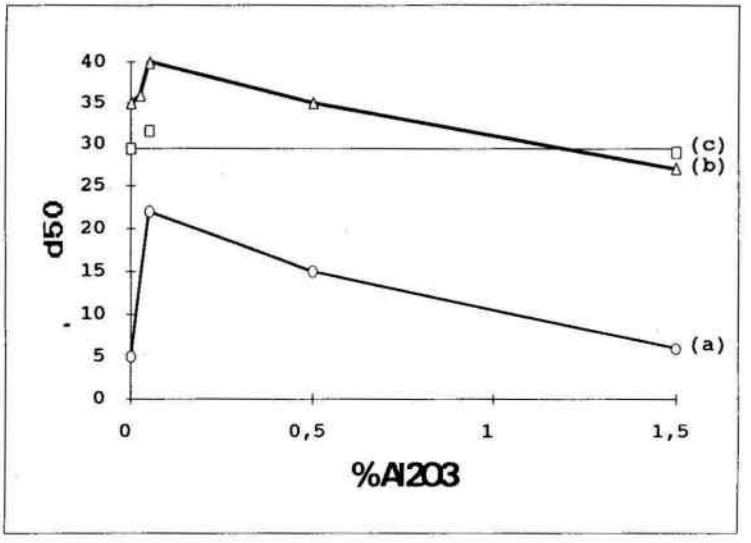

Figure 6. Aluminum effect on d_{50} of gypsum crystals: (a) "0" saturation (Rocha e Ciminelli, 1990) (b) 0,25 saturation (Leão e Ciminelli, 1992); (c) 0,87 saturation.

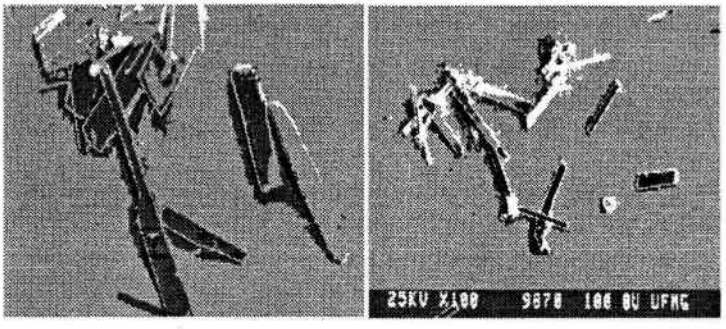

Figure 7. Gypsum crystals precipitated on presence of Al_2O_3 at 0,25 saturation. (a) 0,05%, (b) 1,5%.

Equation (9) and (20) present the relationship between stationary nucleation rate and supersaturation.

$$J(s) = A'Sexp[16v_a^2\sigma^3)/(3RTln^2S) \qquad (9)$$

$$J(s) = A'Sexp[16v_a^2\sigma^3)/(3RTlnS) \qquad (20)$$

These equations show that for homogeneous nucleation (equation (9)), the nucleation rate changes with the square of supersaturation while for heterogeneous nucleation (equation (20)) this relation is linear. Considering that the total nucleation rate is the sum of the homogeneous nucleation (J_{Homo}), heterogeneous nucleation (J_{hete}) and secondary nucleation (J_{sec}) terms, one may written:

$$J = J_{homo} + J_{hete} + J_{sec} \qquad (23)$$

In tests carried out with addition of seeds at t = 0, complete solubilization was observed. The effect of seeds, instead of providing a host substrate for crystals growth, was to increase the calcium sulfate levels in the reactor. This situation favored homogeneous nucleation. The effect of impurities in crystals habit became quite evident since the global nucleation rate was more sensitive to the supersaturation (J changes with the square of S).

When the supersaturation level is increased, the seeds do not completely dissolve, the term J_{homo} becomes less important, and the changes in supersaturation caused by impurities showed a minor effect on global nucleation rate and in crystal sizes. In figure 6 (c), the conditions favored secondary nucleation and the crystals display different characteristics related to those precipitated under conditions that favored primary nucleation. In industrial practice (continuous operation) it is expected the secondary nucleation to predominate. In this case, the impurities are expected to play a minor role on nucleation. Their effects are possibly associated to other phenomena, like agglomeration.

Conclusions:

The effect of impurities on gypsum crystal habit was correlated to their influence on supersaturation. In batch systems, the results indicate a reaction rate more sensitive to supersaturation, J changes with the square of S, as expected when primary nucleation prevails. The effect of impurities was not so evident when the experiments were carried out in continuous MSMPR reactors; in this case the mechanism is likely to be dominated by secondary nucleation .

References:

1 - Budz, J.; Jones A. G. and Mullin J. W. Effect of Selected Impurities on the Continuous Precipitation on Calcium Sulphate (Gypsum). Journal of Chemical Technology and Biotechnology, 1986, vol. 36 p. 153.

2 - Leão, V. A. e Ciminelli, V. S. T. The Effect of Impurities on Gypsum Precipitation. Tecnologia Mineral I, parte B, Ciminelli V. S. T.& Salum, M., J., G. (Eds), ABTM, 1992, p.412 (in Portuguese).

3 - Van Rosmalen, G.; Witkamp, G., J. Industrial Crystallization an Precipitation, Part D (Lecture Notes) p.1. Instituto de Pesquisas Tecnológicas do Estado de São Paulo, IPT, São Paulo, 1992.

4 - Leão, V. A.; Ciminelli, V. S. T., Rocha, S. D. F. Organic Additives on Gypsum Precipitation. Chemical Metallurgy. vol. 3. Proceedings of "IV Meeting of Southern Hemisphere on Mineral Technology". I. Wiekomisky; Sánches, M.; Hecker, C. (Eds)., 1994, p. 243.

5 - Rocha, S. D. F. and Ciminelli, V. S. T. Study of Calcium Sulfate Precipitation in Phosphoric Acid Solutions, Proceedings of the "V Encontro Nacional de Rocha Fosfática". IBRAFOS, São Paulo, S.P., 1991, p 393.

6 - Rocha, S. D. F. and Ciminelli, V. S. T. Effect of Surfactants on the Calcium Sulfate Crystallization in Phosphoric Acid Solutions. Minerals and Metallurgical Processing (in Press), 1994.

7 - Bukart, L.; Voigt, J. Aqueous Precipitation in Hydrometallurgy. In.: Hydrometallurgical Reactor Design and Kinetics, Proceedings..., AIME, PA, USA, 1986, p 441.

8 - Cocheci, V.; Rosca. B.Contributions to the Study of Phosphogypsum Filtration Optimization in Phosphoric Acid Industry. I - The Influence of Impurities on Cristallin Habit of Calcium Sulfate. Buletinul Stiinnui si Technic al institutului Polytechinic "Train Vuia". Timisoara, v. 27, n. 41, 1982, p .1.

9 - He, S.; Oddo, J., E. Tomson, M. B. The Seeded Growth of Calcium Sulfate Dihydrate Crystals in NaCl solutions up to 6 m and 90 ^{0}C. Journal of Colloid and Interface Science, 163, n.2. Mar, 1994, p. 372.

10 - He, S.; Oddo, J., E. Tomson, M. B. The Nucleation Kinetics of Calcium Sulfate Dihydrate in NaCl solutions up to 6 m and 90 ^{0}C. Journal of Colloid and Interface Science, 162 n.2. Fev., 1994, p. 297.